photonics

MDPI

Communication

Extending the Imaging Depth of Field through Scattering Media by Wavefront Shaping of Non-Diffraction Beams

Tongyu Han [1,2], Tong Peng [2], Runze Li [2], Kaige Wang [1,*], Dan Sun [1] and Baoli Yao [2,*]

[1] National Center for International Research of Photoelectric Technology & Nano-Functional Materials and Application, Shaanxi Provincial Key Laboratory of Photoelectric Technology, Institute of Photonics and Photon-Technology, Northwest University, Xi'an 710127, China
[2] State Key Laboratory of Transient Optics and Photonics, Xi'an Institute of Optics and Precision Mechanics, Chinese Academy of Sciences, Xi'an 710119, China
* Correspondence: wangkg@nwu.edu.cn (K.W.); yaobl@opt.ac.cn (B.Y.)

Abstract: Increasing the depth of field (DOF) is a crucial issue for imaging through scattering media. In this paper, an improved genetic algorithm is used to modulate the wavefront of light through scattering media, by which high-quality refocusing and imaging through scattering media are achieved. Then, the DOF of the imaging system is effectively extended by further modulating the refocused beam into a non-diffraction beam. Two kinds of non-diffraction beams, i.e., a Bessel beam and Airy beam, were produced as a demonstration. The experimental results show that compared to the Gaussian beam, the DOF of the imaging system by combining the wavefront shaping and non-diffraction Bessel beam or Airy beam can be improved by a factor of 1.1 or 1.5, respectively. The proposed method is helpful for the technical development of high-quality imaging through scattering media with a large DOF.

Keywords: imaging through scattering media; wavefront shaping; depth of field; interleaved segment correction; non-diffraction beam

Citation: Han, T.; Peng, T.; Li, R.; Wang, K.; Sun, D.; Yao, B. Extending the Imaging Depth of Field through Scattering Media by Wavefront Shaping of Non-Diffraction Beams. *Photonics* **2023**, *10*, 497. https://doi.org/10.3390/photonics10050497

Received: 31 March 2023
Revised: 23 April 2023
Accepted: 24 April 2023
Published: 26 April 2023

1. Introduction

Optical imaging is one of the most important pathways for directly obtaining information on nature. Unfortunately, light is scattered when it propagates in inhomogeneous media, such as fog, turbid water, biological tissue, and so on. Incident light waves that encounter particles that have a wavelength size in the scattering media will cause a high distortion of the wavefront and form random speckles. The random light wave makes imaging impossible.

Up to now, techniques such as wavefront shaping [1,2], transmission matrix (TM) measurement [3], adaptive optics [4–6], and speckle correlation method [7] have been developed to overcome this limitation and realize imaging through scattering media. However, challenges still exist, and the imaging depth of field (DOF) is always limited. The input and output imaging relationship can be obtained by measuring the TM of the scattering media, and then imaging of objects can be achieved behind scattering media by calculating the inverse transmission. However, the TM of a single transverse plane is usually measured; thus, only objects on the plane can be imaged. Furthermore, the method requires a huge calculation and time to measure the TM of different axial planes to recover images at an extended depth. The speckle correlation method can recover the image by calculating the autocorrelation or cross-correlation of the speckles. It also works in a limited DOF range because the speckles' correlation decreases as the imaging depth is changed. To extend the imaging DOF, many efforts have been made. Takasaki [8] employed the phase-space analysis method to locate the depth of a point source behind the scattering media to extend the DOF. Antipa [9] developed a Diffuser-Cam method by capturing a series of speckle intensities and solving the inverse imaging problem through a compressed

sensing algorithm to achieve 3D imaging with a large DOF. Xin [10] established a wavefront recovery model based on a light-field estimation to obtain a speckle intensity distribution by integration to extend the DOF. Liao [11] enlarged the DOF by combining point spread functions (PSFs) of different depths in the speckle correlation method. Although these methods can extend the DOF, massive measurements and data processes are needed, and the DOFs are usually discontinuous and separated in dispersed depth ranges.

Compared with the aforementioned methods, wavefront shaping achieves refocusing and imaging through scattering media by employing optoelectronic devices to compensate for the wavefront distortion [12]. As compared to alternative optoelectronic devices [13,14], the spatial light modulator (SLM) [15,16] has the advantages of a high spatial resolution, high energy utilization, and high modulation depth, which can correct the distortion caused by scattering with a high precision. The proper correction phase can be obtained by directly measuring the wavefront distortion with the help of a guide star [17] or by searching loops with intensity feedback [18]. The point-to-point imaging relationship through scattering media was rebuilt after each pixel of SLM found its optimal correction phase [19]. However, the imaging DOF is also confined to the near focal plane due to the diffraction of light. Objects departing from the focal plane will result in a blurred image because of the divergency of the Gaussian beam. Recently, it has been proven that non-diffraction beams (such as a Bessel beam, Airy beam, Mathieu beam, etc.) can be used to expand the imaging DOF [20]. The center energy of these beams is relatively concentrated within a long range during propagation, i.e., the non-diffraction property [21,22]. Thus, the imaging quality can be maintained within a longer range than a Gaussian beam [23,24]. Multiple detections of the PSFs at different positions are unnecessary when extending the DOF via non-diffraction beams, and the whole extended depth images can be directly obtained in a single shot.

In this paper, the DOF of imaging through scattering media is extended by wavefront shaping and non-diffraction beams. An improved genetic algorithm (GA), or namely the interleaved segment correction (ISC), was used to search for the correction phase to compensate for wavefront distortion. Thus, the scattered light can be refocused, and the imaging of objects behind the scattering media is demonstrated. To extend the DOF, the refocused light was further shaped into non-diffraction beams, i.e., a Bessel beam and Airy beam. Both coherent and incoherent illuminations were verified. Compared to a Gaussian beam, the DOF of an Airy beam was improved by a factor of 1.5 under coherent illumination, and under incoherent illumination, the DOFs were improved by a factor of 1.1 and 1.5 by a Bessel beam and Airy beam, respectively.

2. Materials and Methods

2.1. Principle

The principle of wavefront shaping is illustrated in Figure 1. In a traditional imaging system (for example, a single-lens imaging system), a point light source converges into focus on the image plane through the lens (Figure 1a). The wavefront of the light beam is distorted after passing through a scattering media and forms speckles (Figure 1b). Refocusing and imaging through scattering media can be realized if the wavefront distortion is compensated by using a light-field modulation technology, such as a spatial light modulator (SLM) addressing a scatter inversed phase (Figure 1c). The focus of the Gaussian beam diverges from the focal plane, and the imaging DOF is limited. Extending the DOF can be achieved by non-diffraction beams, as this can maintain the intensity of the central lobe within a long range (Figure 1d). The extending DOF imaging through scattering media contains two steps, the wavefront shaping for correcting the distortion and the non-diffraction beam modulation.

The imaging result of the coherent condition is the convolution of the object and the PSF of the system within the memory effect [25] range of the scattering medium:

$$I(x) = \left| \int O(x - \Delta x) \cdot PSF(x) d\Delta x \right|^2 = |O * PSF|^2, \quad (1)$$

where $O(x)$ represents the object and Δx represents the displacement. The scattering media diffused the PSF, resulting in random speckles. If the distortions of the wavefront caused by the scattering medium are corrected by SLM, the speckles can be transferred into a focus, i.e., the PSF of the system is corrected into a point-like function. The object within the memory effect can also be imaged through the scattering medium, as shown in Figure 1c.

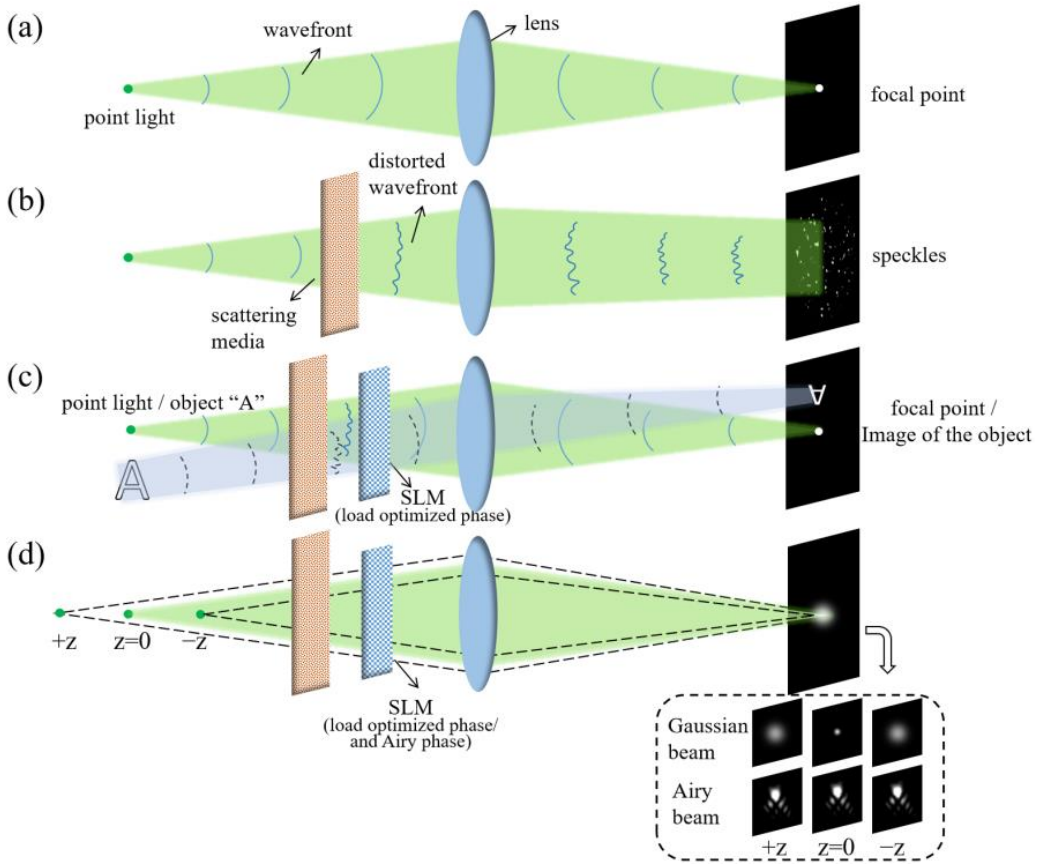

Figure 1. The principle of wavefront shaping and DOF extension. (**a**) The beam is focused by a lens; (**b**) the beam is transformed into speckles due to wavefront distortions caused by scattering media; (**c**) the scattered beam is corrected by wavefront shaping to achieve refocusing and imaging through scattering media; (**d**) the imaging DOF is extended by non-diffraction beams.

The key point of wavefront shaping is to obtain the proper compensation phase to correct the distortions of light. In this work, an improved GA with fast convergence, namely interleaved segment correction (ISC-GA) [26], is employed to acquire the compensation phase. Unlike the traditional GA, which uses all the units on the SLM at the same time, the ISC-GA divides all the pixels of the SLM into multiple groups; for each group, one can obtain an optimal phase that can refocus the scattered light, and by superimposing all phases of each group, the final optimal phase is acquired. Take four groups for example, as shown in Figure 2, the pixels of SLM are divided into four groups of interleaved segment regions (Figure 2a), and each region contains multiple pixels (Figure 2b). Take the intensity of one pixel or several pixels of the CCD camera as feedback; by performing the GA for each group independently, four corrected phases can be obtained (Figure 2c). The final compensation phase is acquired by combining the phases of four groups (Figure 2d). It is worth emphasizing that in order to provide a common reference for interference, the other three non-correcting groups are kept at zero phases on all of their segments when one group is optimized. Therefore, the four different groups' optimization processes are carried out using the same reference, ensuring a constructive interference at the target when the final combined phase is applied. One more thing to note is that in Figure 2, only

four groups are selected to illustrate the principle of ISC. If a higher accuracy is required in practice, the SLM can be divided into many more groups.

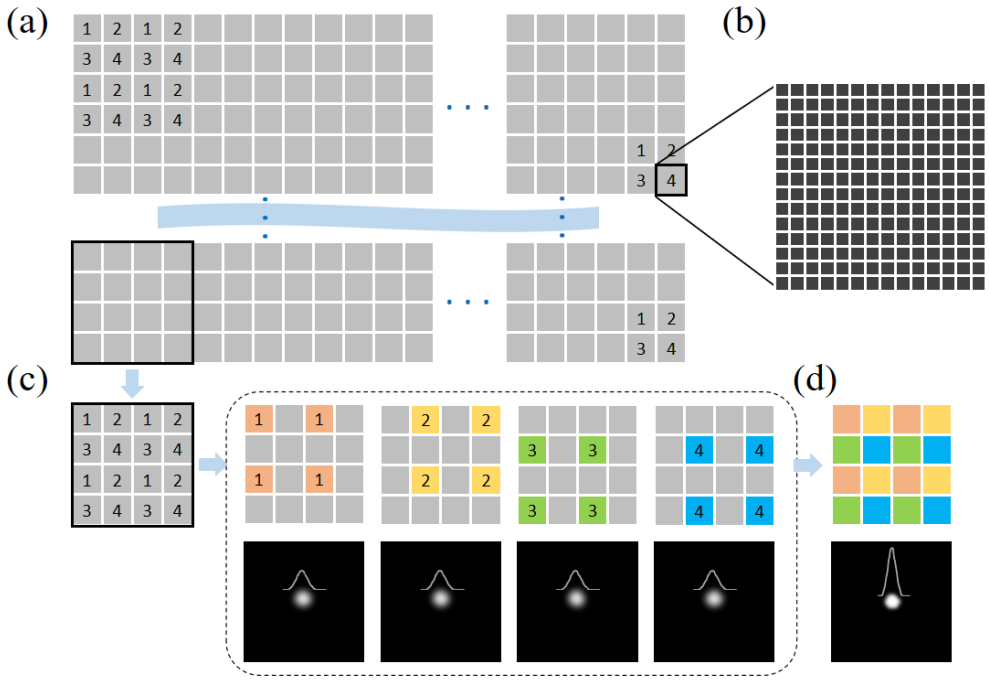

Figure 2. Principle of the ISC method. (**a**) The pixel array of an SLM is divided into four interleaved segments; (**b**) multiple pixels are included in each segment; (**c**) segments marked with different colors are modulated separately in sequence to obtain the partitioned phase patterns; (**d**) the optimal phase pattern is acquired by a combination of the partitioned phase patterns.

To generate the non-diffraction beam through scattering media, the correction phase and the phase mask for the non-diffraction beam are superimposed, which can be calculated by:

$$\varphi = \text{angle}\left(A_1 e^{i\varphi_1} + A_2 e^{i\varphi_2}\right) \approx \varphi_1 + \varphi_2, \quad (2)$$

where $A_1 e^{i\varphi_1}$ is the correction phase for compensating scattering and $A_2 e^{i\varphi_2}$ is the phase for generating a non-diffraction beam.

2.2. Experimental Setup

The experimental setup is shown in Figure 3, which contains two parts: the wavefront shaping part in Figure 3a and the imaging through scattering media part in Figure 3b. The two parts can be switched by turning the flipping mirror M3.

For wavefront shaping, as shown in Figure 3a, a laser beam (λ = 532 nm) is firstly expanded and collimated by lens 1 (L1, f = 50 mm) and lens 2 (L2, f = 150 mm), before passing through a horizontal polarizer (P) and a beam splitter prism (BS1) and falling incident onto the SLM (1920 × 1080 pixels, pixel size 8 μm, PLUTO-II-VIS, HoloEye Inc., Berlin, Germany) for modulation. The light beam is modulated by the SLM and illuminates the scattering medium (S, DG10-600-MD, Thorlabs) through lens 3 (L3, f = 30 mm) and lens 4 (L4, f = 150 mm). The output speckles are collected by CCD1 (1280 × 960 pixels, pixel size 3.75 μm, 8-bit, DMK 23U445, The Imaging Source Inc., Bremen, Germany). In the wavefront shaping process, CCD1 is employed to monitor the speckle field and provide feedback to the ISC method. With the feedback optimization, the correction phase can be obtained, and the light speckle is focused. It should be noted that the position of the SLM should be conjugated with the scattering medium to make good use of the memory effect

range [7]. If the state of the scattering medium changes, the wavefront distortion needs to be re-corrected.

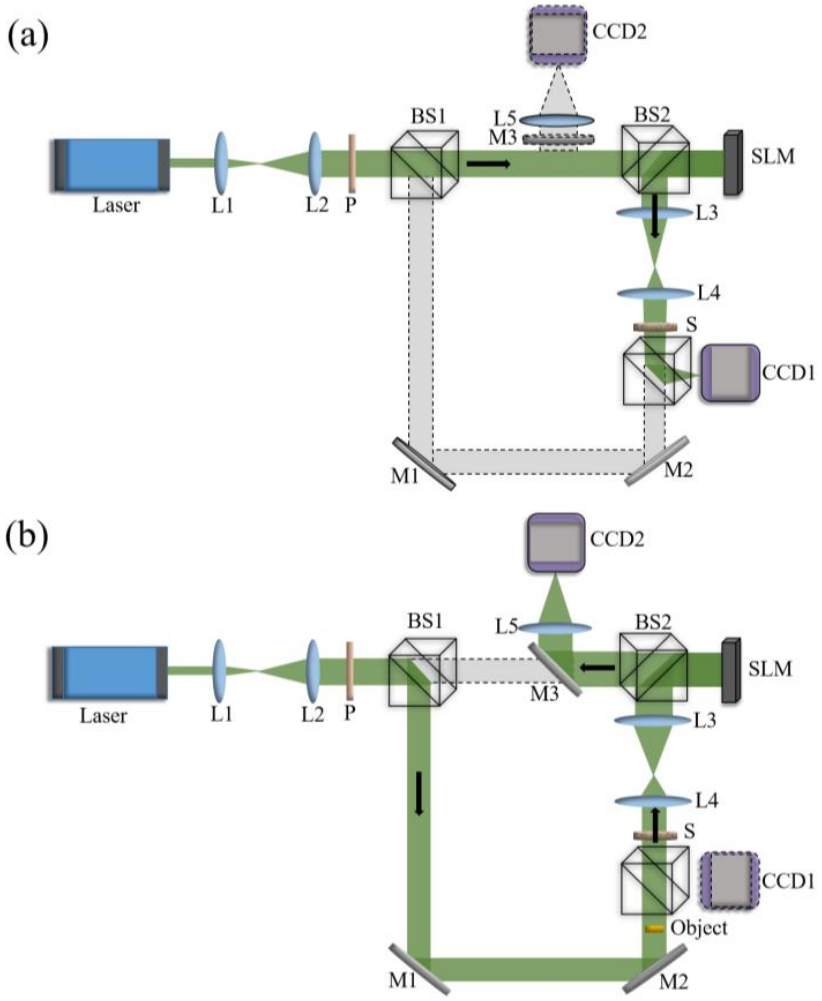

Figure 3. Schematic diagram of the experimental setup. (**a**) The optical path for wavefront shaping; (**b**) the optical path for imaging through scattering media. L: lens, P: horizontal polarizer, BS: beam-splitter prism, M: mirror, S: scattering medium.

Once the distortion of the wavefront is corrected, real-time imaging through scattering media can be realized. The imaging part is illustrated in Figure 3b, where the light beam reflected by BS1, M1, and M2 illuminates the object (USAF 1951). The light speckles output from the scattering medium, relayed by lens 4 and lens 3, and then are incident onto the SLM for correction. Due to the reversibility of the optical path, when the SLM addresses the previously found correction phase, images of the object can be captured by CCD2 (1280 × 960 pixels, pixel size 3.75 μm, 8 bit, DMK 23U445, The Imaging Source Inc., Bremen, Germany) through BS1, M3, and lens 5 (L5, f = 200 mm). During the experiment, the calibration patterns are generated using 1080 × 1080 SLM pixels that are divided into 90 × 90 segments, each of which consists of 12 × 12 pixels. In the ISC-GA method, 90 × 90 segments are separated into nine groups of interlaced 30 × 30 segments.

3. Results

The focusing results are shown in Figure 4, where Figure 4a is the random speckle pattern on CCD1 before wavefront correction. With the optimal correction phase (Figure 4b), the speckles are refocused with a peak-to-background ratio (PBR) of 980, as shown in Figure 4c. To extend the imaging DOF, the Gaussian focus is modulated by superpos-

ing the optimal correction phase with the phase of the non-diffraction beam, as shown in Figure 4d,e. The corresponding Bessel beam and Airy beam are generated through scattering media, as shown in Figure 4f,g, respectively.

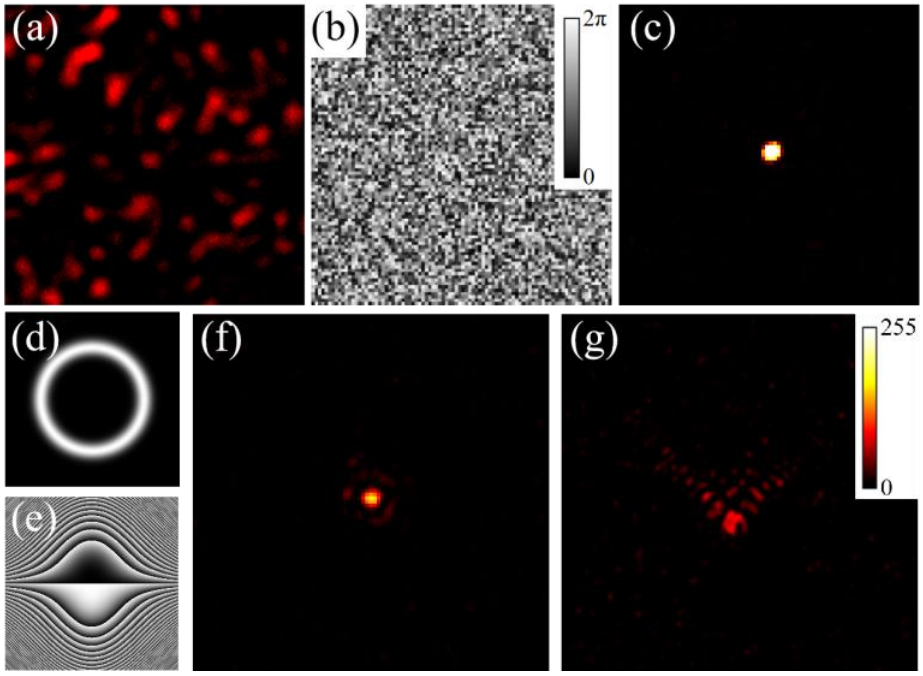

Figure 4. (**a**) Speckles before wavefront correction; (**b**) the correction phase found by ISC-GA; (**c**) the refocusing of the speckles after wavefront correction; (**d**,**e**) the phase for generating the Bessel beam and Airy beam; (**f**,**g**) the generated Bessel beam and Airy beam behind the scattering media.

To demonstrate the extended imaging DOF by a non-diffraction beam through scattering media, the object was fixed on an axial moving stage (KMTS50E/M) that moved across the focal plane. The number "2" on the USAF 1951 was selected for imaging. The imaging results at different axial positions are shown in Figure 5, where Figure 5a shows the imaging results of a Gaussian beam and Airy beam. We take the opposite direction of light propagation as the forward direction of the coordinate. To quantitatively evaluate the DOF of the imaging, the Pearson correlation coefficients (PCCs) of the imaging results in different positions are calculated with the original object and are shown in Figure 5b. The optimal imaging plane under the Gaussian beam is at the focal plane (the position of 0 mm), and the image quality decreases rapidly when the target moves away from the focal plane. We defined the DOF as the range of PCC above 0.5, which is about 27 mm for a Gaussian beam. The imaging quality of the Airy beam is worse than the Gaussian beam at the focal plane, mainly because the side lobes of the Airy beam take away the focus intensity and decrease the imaging quality. However, the PCC of the Airy beam decreases slower than the Gaussian beam when the target moves away from the focal plane. The range of PCC above 0.5 is about 41 mm for the Airy beam, which is about 1.5 times that of the Gaussian beam.

Further, the structural similarity index measure [27] (SSIM) with the original object and the Peak Signal-to-Noise Ratio [28] (PSNR) of the imaging results are also given for the imaging quality comparison between the Gaussian beam and Airy beam, as shown in Figure 5c,d. The SSIM and PSNR show the same tendency as PCC. It should be noted that the imaging magnification is changed as the object moves along the axis; thus, the original object is also tuned accordingly to calculate the exact PCC and SSIM value. In fact, the imaging quality is limited under a coherent light illumination [19], and the coherent speckles evidently exist in Figure 5. Therefore, we then investigated the imaging under an incoherent light illumination.

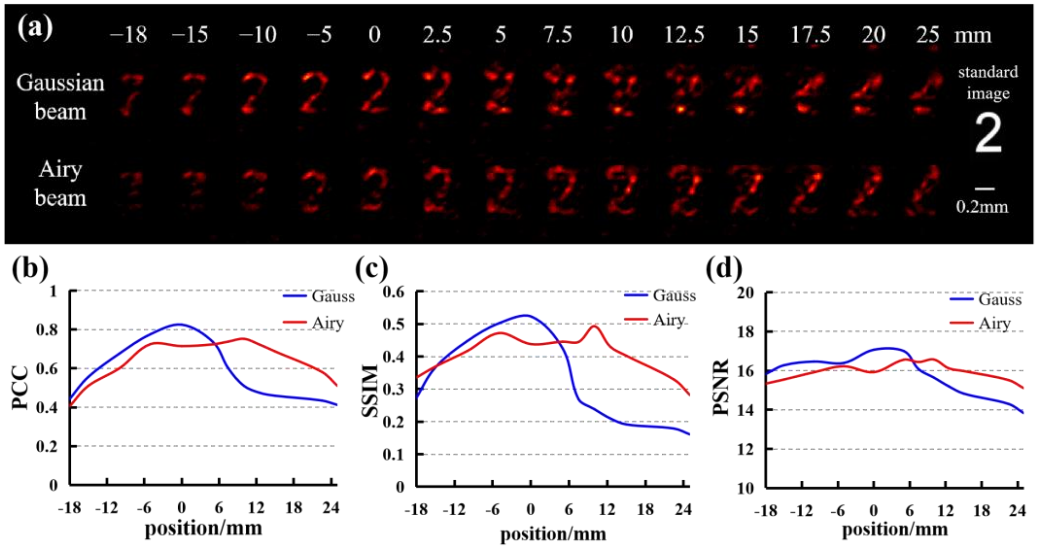

Figure 5. Extended DOF with Airy beam in coherent illumination. (**a**) The standard image and images along the axis at various distances; (**b**,**c**) PCC and SSIM profiles comparing the images and using the original object; (**d**) PSNR of the imaging results.

For an incoherent light illumination condition, a rotating ground glass is introduced in the optical path before the object [29]. Figure 6a shows the imaging results of the target through scattering media. A Bessel beam and Airy beam are used to extend the imaging DOF. It can be seen that under incoherent illumination, the speckles are reduced, and the PCC of the Gaussian beam can reach above 0.9 at the focal plane. Same as the results under coherent illumination, the imaging quality of the non-diffraction Bessel beam and Airy beam can be maintained within a longer axial range. The PCC, SSIM, and PSNR are provided in Figure 6b–d. The range of PCC above 0.5 is about 14.5 mm for the Gaussian beam, 16 mm for the Bessel beam, and 21.5 mm for the Airy beam, respectively. As a result of this, the DOF increased about 1.1 times and 1.5 times, respectively.

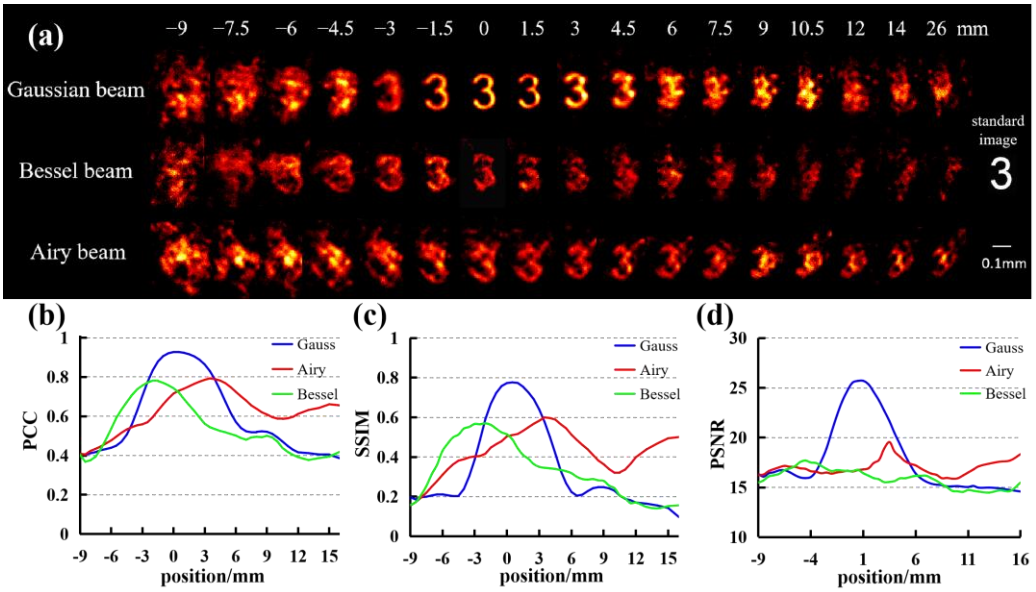

Figure 6. Extended DOF with Airy beam and Bessel beam under incoherent illumination. (**a**) The standard image and images along the axis at various distances; (**b**,**c**) PCC and SSIM profiles comparing the images and using the original object; (**d**) PSNR of the imaging results.

4. Discussion

From the results shown in Figure 4, it can be seen that the ISC method can effectively improve the refocusing quality through the scattering medium, and the PBR value can break through the dynamic range limit of CCD, which is fundamental for achieving clear imaging and extending the depth of field. The results of Figures 5 and 6 show that the DOF of imaging through scattering media can be effectively extended by combining wavefront shaping with a non-diffraction beam. The imaging DOFs are influenced by both the wavefront-shaping quality and non-diffraction-beam properties. The Bessel beam extends the DOF along the negative axis, while the Airy beam extends the DOF along the positive axis. This is because the wavefront distortion caused by scattering is compensated by using wavefront shaping, but it is not fundamentally eliminated. Therefore, the generated Bessel beam and Airy beam are both affected, and the performances are not as good as that obtained in systems without scattering media. High-precision wavefront shaping by increasing the used SLM segment number can further increase the imaging quality and DOF, but on the other hand, more time is needed.

The side lobes of the Bessel beam and Airy beam markedly reduce the imaging quality, decreasing the energy of the main lobe and generating background noise. In follow-up research, in order to increase the imaging quality via non-diffraction beams, the polarization state of the light field could be modulated to recover the polarization-state information of the object light. Additionally, deconvolution could be applied to reduce the influence of side lobes, or a needle-shaped beam with fewer side lobes could be used for imaging.

5. Conclusions

In this paper, the wavefront-shaping method of interleaved segment correction (ISC) is introduced to compensate for the wavefront distortion caused by scattering media. A refocusing of the light behind the scattering media is realized. With the memory effect of the media, the imaging of the objects through scattering media is achieved. By superimposing the compensation phase and the non-diffraction-beam phase, two non-diffraction beams, i.e., a Bessel beam and Airy beam, are generated behind scattering media. Then, the imaging DOF is extended with the two non-diffraction beams. The proposed method may have potential applications in astronomical observations, biological imaging, and some related fields.

Author Contributions: Conceptualization, T.H., T.P. and R.L.; methodology, T.H. and T.P.; software, T.H., T.P. and R.L.; validation, T.H., T.P. and R.L.; formal analysis, T.H.; investigation, T.H.; resources, T.P., K.W., D.S. and B.Y.; data curation, T.H.; writing—original draft preparation, T.H.; writing—review and editing, all authors; visualization, T.H.; supervision, all authors; project administration, K.W., D.S. and B.Y.; funding acquisition, K.W. All authors have read and agreed to the published version of the manuscript.

Funding: This research was supported by the National Natural Science Foundation of China (No. 62105359, 62275216, 61775181), the National key scientific instrument and equipment development projects of China (No. 51927804), the China Postdoctoral Science Foundation (Grant No. 2020M673522), the Innovation Capability Support Program of Shaanxi Province (Grant No. S2018-ZC-TD-0061, TZ0393), the State Key Laboratory of Transient Optics and Photonics, Chinese Academy of Sciences (SKLST202109), and the Key research and development program of Shaanxi Province (Grant No. 2022SF-087, 2021GY-079).

Institutional Review Board Statement: Not applicable.

Informed Consent Statement: Not applicable.

Data Availability Statement: Not applicable.

Conflicts of Interest: The authors declare no conflict of interest.

References

1. Hong, P.; Ojambati, O.S.; Lagendijk, A.; Mosk, A.P.; Vos, W.L. Three-dimensional spatially resolved optical energy density enhanced by wavefront shaping. *Optica* **2018**, *5*, 844–849. [CrossRef]
2. Yaqood, Z.; Psaltis, D.; Feld, M.S.; Yang, C. Optical phase conjugation for turbidity suppression in biological samples. *Nat. Photon.* **2008**, *2*, 110–115.
3. Popoff, S.M.; Lerosey, G.; Fink, M.; Boccara, A.C.; Gigan, S. Controlling Light Through Optical Disordered Media: Transmission Matrix Approach. *New J. Phys.* **2011**, *13*, 123021. [CrossRef]
4. Wang, K.; Sun, W.; Richie, C.T.; Harvey, B.K.; Betzig, E.; Ji, N. Direct wavefront sensing for high-resolution in vivo imaging in scattering tissue. *Nat. Commun.* **2015**, *6*, 7276. [CrossRef]
5. Hampson, K.M.; Turcotte, R.; Miller, D.T.; Kurokawa, K.; Males, J.R.; Ji, N.; Booth, M.J. Adaptive optics for high-resolution imaging. *Nat. Rev. Methods Prim.* **2021**, *1*, 68. [CrossRef]
6. Chen, C.; Jones, S.M.; Silva, D.A.; Olivier, S.S. High-Resolution Adaptive Optics Scanning Laser Ophthalmoscope with Dual Deformable Mirrors. *J. Opt. Soc. Am. A.* **2006**, *24*, 1305–1312. [CrossRef]
7. Katz, O.; Heidmann, P.; Fink, M.; Gigan, S. Non-invasive real-time imaging through scattering layers and around corners via speckle correlations. *Nat. Photon.* **2014**, *8*, 784–790. [CrossRef]
8. Takasaki, K.T.; Fleischer, J.W. Phase-space measurement for depth-resolved memory-effect imaging. *Opt. Express* **2014**, *22*, 31426–31433. [CrossRef] [PubMed]
9. Antipa, N.; Kuo, G.; Heckel, R.; Mildenhall, B.; Bostan, E.; Ng, R.; Waller, L. DiffuserCam: Lensless single-exposure 3D imaging. *Optica* **2018**, *5*, 1–9. [CrossRef]
10. Xin, J.; Wang, Z.; Wang, X.; Dai, Q. Depth of field extended scattering imaging by light field estimation. *Opt. Lett.* **2018**, *43*, 4871–4874.
11. Liao, M.; Lu, D.; Pedrini, G.; Osten, W.; Situ, G.; He, W.; Peng, X. Extending the depth-of-field of imaging systems with a scattering diffuser. *Sci. Rep.* **2019**, *9*, 7165–7172. [CrossRef]
12. Vellekoop, I.M.; Mosk, A.P. Focusing coherent light through opaque strongly scattering media. *Opt. Lett.* **2007**, *32*, 2309–2311. [CrossRef]
13. Stockbridge, C.; Lu, Y.; Moore, J.; Hoffman, S.; Paxman, R.; Toussaint, K.; Bifano, T. Focusing through dynamic scattering media. *Opt. Express* **2012**, *20*, 15086–15092. [CrossRef]
14. Galaktionov, I.; Sheldakova, J.; Nikitin, A.; Samarkin, V.; Parfenov, V.; Kudryashov, A. Laser beam focusing through a moderately scattering medium using bimorph mirror. *Opt. Express* **2020**, *28*, 38061–38075. [CrossRef]
15. He, C.; Shen, Y.; Forbes, A. Towards higher-dimensional structured light. *Light Sci. Appl.* **2022**, *11*, 205. [CrossRef]
16. Galaktionov, I.; Nikitin, A.; Sheldakova, J.; Toporovsky, V.; Kudryashov, A. Focusing of a Laser Beam Passed through a Moderately Scattering Medium Using Phase-Only Spatial Light Modulator. *Photonics* **2022**, *9*, 296. [CrossRef]
17. Horstmeyer, R.; Ruan, H.; Yang, C. Guidestar-assisted wavefront-shaping methods for focusing light into biological tissue. *Nat. Photon.* **2015**, *9*, 563–571. [CrossRef]
18. Vellekoop, I.M.; Mosk, A.P. Phase control algorithms for focusing light through turbid media. *Opt. Commun.* **2008**, *281*, 3071–3080. [CrossRef]
19. Katz, O.; Small, E.; Silberberg, Y. Looking around corners and through thin turbid layers in real time with scattered incoherent light. *Nat. Photon.* **2012**, *6*, 549–553. [CrossRef]
20. Mikula, G.; Kolodziejczyk, A.; Makowski, M.; Prokopowicz, C.; Sypeket, M. Diffractive elements for imaging with extended depth of focus. *Opt. Eng.* **2005**, *44*, 058001. [CrossRef]
21. Durnin, J.J.J.M.; Miceli, J.J., Jr.; Eberly, J.H. Diffraction-free beams. *Phys. Rev. Lett.* **1987**, *58*, 1499–1501. [CrossRef] [PubMed]
22. Vasara, A.; Turunen, J.; Friberg, A.T. Realization of general nondiffracting beams with computer-generated holograms. *J. Opt. Soc. Am. A.* **1989**, *6*, 1748–1754. [CrossRef] [PubMed]
23. Hu, Y.; Chen, Z.; Xiang, L.; Xing, D. Extended depth-of-field all-optical photoacoustic microscopy with a dual non-diffracting Bessel beam. *Opt. Lett.* **2019**, *44*, 1634–1637. [CrossRef] [PubMed]
24. Planchon, T.A.; Gao, L.; Milkie, D.E.; Davidson, M.W.; Galbraith, J.A.; Galbraith, C.G.; Betzig, E. Rapid three-dimensional isotropic imaging of living cells using Bessel beam plane illumination. *Nat. Meth.* **2011**, *8*, 417–423. [CrossRef]
25. Freund, I.I.; Rosenbluh, M.; Feng, S. Memory effects in propagation of optical waves through disordered media. *Phys. Rev. Lett.* **1988**, *61*, 2328–2331. [CrossRef]
26. Li, R.; Peng, T.; Liang, Y.; Yang, Y.; Yao, B.; Yu, X.; Min, J.; Lei, M.; Yan, S.; Zhang, C.; et al. Interleaved segment correction achieves higher improvement factors in using genetic algorithm to optimize light focusing through scattering media. *J. Opt.* **2017**, *19*, 105602. [CrossRef]
27. Wang, Z.; Bovik, A.C.; Sheikh, H.R.; Simoncelli, E.P. Image quality assessment: From error visibility to structural similarity. *IEEE T. Image Process.* **2004**, *13*, 600–612. [CrossRef]

28. Huynh-Thu, Q.; Ghanbari, M. Scope of validity of PSNR in image/video quality assessment. *Electron. Lett.* **2008**, *44*, 800–801. [CrossRef]
29. Somekh, M.G.; See, C.W.; Goh, J. Wide field amplitude and phase confocal microscope with speckle illumination. *Opt. Commun.* **2000**, *174*, 75–80. [CrossRef]